AD-A160 561 STS (SPACE TRANSPORTATION SYSTEM) LAUNCH-INDUCED VIBRATION FORECASTS FOR VANDENBERG AFB(U) AIR FORCE GEOPHYSICS LAB HANSCOM AFB MA J C BATTIS 07 OCT 85 1/1

UNCLASSIFIED AFGL-TR-85-0227 F/G 16/1 NL

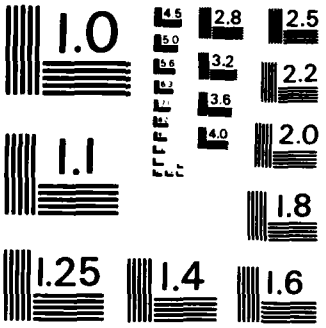

MICROCOPY RESOLUTION TEST CHART
NATIONAL BUREAU OF STANDARDS-1963-A

AFGL-TR-85-0227

STS LAUNCH-INDUCED VIBRATION FORECASTS FOR VANDENBERG AFB

J. C. Battis
Air Force Geophysics Laboratory
Hanscom AFB, Massachusetts

Abstract

Launch-induced vibration environment forecasts have been made for locations in major Ground Support System (GSS) structures at the Vandenberg AFB Shuttle launch facility (V23). These forecasts were made by coupling a model for the Shuttle rocket acoustics with observed vibrations of GSS structures due to charge detonations over the Launch Mount. The forecasts indicate that launch environments at two locations will exceed levels of concern established for this study. First, the potential exists for pounding between the Payload Changeout Room (PCR) and the transfer tower of the Payload Preparation Room (PPR). Second, accelerations exceeding 1 g are forecast for the floor of the Orbiter Functional Simulator Room (OFS) in the Administration Building (AB). At all other locations motion levels were found to be significantly below the criteria established for the respective sites.

I. Introduction

The Air Force Space Division (SD) has established a requirement to forecast the vibro-acoustic environment for the Space Transportation System (STS) launches at V23, the Vandenberg AFB Shuttle launch facility. These forecasts would be used to aid design, operational planning and lifetime projections for the facility. Existing data were inadequate to describe the phasing of pressure loads on the structures at V23, an essential property for estimating the induced vibrations of structures.

This paper covers one phase of a comprehensive study undertaken to provide the required forecasts. In particular, the motion predictions for three of the GSS facilities located near the pad are discussed. Other elements of this study included the development of a model for the STS rocket acoustic emissions[1,2] and forecasts of the acoustic environment at V23[3].

II. The Launch Facility

Figure 1 shows a plan view of the Vandenberg launch complex, V23. Four major structures are located within 400 meters of the Launch Mount; the Payload Preparation Room (PPR), the Payload Changeout Room (PCR), the Mobile Service Tower (MST), and the Shuttle Assembly Building (SAB). This facility is in sharp contrast with the launch pad area at Kennedy Space Center (KSC) which is essentially located in an open, flat field. The nearest major structure at KSC is located at a distance greater than four kilometers from the pad.

The buildings at V23 range from 55 to 85 meters in height and are primarily steel frame structures. With the exception of the transfer tower, however, the PPR is of concrete construction. The PCR, MST and SAB are mobile allowing the buildings to move up to the Launch Mount. As shown in Figure 1 they are in launch configuration.

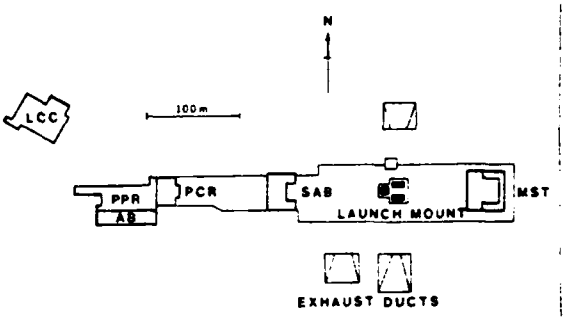

Fig. 1 Major structures at V23.

The close proximity of these large structures to the Launch Mount is anticipated to greatly alter the acoustic pressure field over the pad area as compared to that observed at KSC. This will result from multipathing and backscattering of the Shuttle acoustics. It is apparent that pressure loading models used for vibration forecasts at V23 can not be based on unmodified acoustic data from simulations of or actual Shuttle launches at KSC.

III. The Simulation Procedure

The launch-induced vibration forecasts presented in this paper were obtained by coupling an acoustic emissions model for a typical Shuttle launch at an open, flat earth site (KSC) with the observed vibrations in V23 facilities due to a series of small charge detonations along a typical Shuttle trajectory. The explicit simulation algorithm can be developed by breaking the Shuttle trajectory into a series of discrete source locations. The theory of linear, time invariant systems is then applied at each discrete source.

Under this development, observed vibrations in the structures due to known pressure sources, such as small charge detonations collocated with the discrete Shuttle sources, can be viewed as system response functions. These response functions incorporate all site particular propagation effects, such as multipathing and backscattering, that define the phasing of loads on the structure and the

Unclassified
SECURITY CLASSIFICATION OF THIS PAGE

REPORT DOCUMENTATION PAGE

1a. REPORT SECURITY CLASSIFICATION: Unclassified	1b. RESTRICTIVE MARKINGS
2a. SECURITY CLASSIFICATION AUTHORITY	3. DISTRIBUTION/AVAILABILITY OF REPORT: Approved for public release; Distribution unlimited.
2b. DECLASSIFICATION/DOWNGRADING SCHEDULE	
4. PERFORMING ORGANIZATION REPORT NUMBER(S): AFGL-TR-85-0227	5. MONITORING ORGANIZATION REPORT NUMBER(S)
6a. NAME OF PERFORMING ORGANIZATION: Air Force Geophysics Laboratory; 6b. OFFICE SYMBOL (If applicable): LWH	7a. NAME OF MONITORING ORGANIZATION
6c. ADDRESS (City, State and ZIP Code): Hanscom AFB, Massachusetts 01731	7b. ADDRESS (City, State and ZIP Code)
8a. NAME OF FUNDING/SPONSORING ORGANIZATION; 8b. OFFICE SYMBOL (If applicable)	9. PROCUREMENT INSTRUMENT IDENTIFICATION NUMBER
8c. ADDRESS (City, State and ZIP Code)	10. SOURCE OF FUNDING NOS.

PROGRAM ELEMENT NO.	PROJECT NO.	TASK NO.	WORK UNIT NO.
62101F	7600	09	05

11. TITLE (Include Security Classification): STS Launch-Induced Vibration Forecasts for Vandenberg AFB

12. PERSONAL AUTHOR(S): James C. Battis

13a. TYPE OF REPORT	13b. TIME COVERED	14. DATE OF REPORT (Yr., Mo., Day)	15. PAGE COUNT
REPRINT	FROM ____ TO ____	1985 October 7	8

16. SUPPLEMENTARY NOTATION: Presented at the AIAA Shuttle Environment and Operations II Meeting, 15 Nov 1985, Houston, TX

17. COSATI CODES		
FIELD	GROUP	SUB. GR.

18. SUBJECT TERMS (Continue on reverse if necessary and identify by block number): STS launch induced vibrations; Vandenberg V23 facility responses; STS vibration forecasts; Acoustic loading

19. ABSTRACT (Continue on reverse if necessary and identify by block number)

Launch induced vibration environment forecasts have been made for locations in major Ground Support System (GSS) structures at the Vandenberg AFB Shuttle launch facility (V23). These forecasts were made by coupling a model for the Shuttle rocket acoustics with observed vibrations of GSS structures due to charge detonations over the Launch Mount. The forecasts indicate that launch environments at two locations will exceed levels of concern established for this study. First, the potential exists for pounding between the Payload Changeout Room (PCR) and the transfer tower of the Payload Preparation Room (PPR). Second, accelerations exceeding 1 g are forecast for the floor of the Orbiter Functional Simulator Room (OFS) in the Administration Building (AB). At all other locations motion levels were found to be significantly below the criteria established for the respective sites.

20. DISTRIBUTION/AVAILABILITY OF ABSTRACT	21. ABSTRACT SECURITY CLASSIFICATION
UNCLASSIFIED/UNLIMITED ☐ SAME AS RPT. ☒ DTIC USERS ☐	Unclassified

22a. NAME OF RESPONSIBLE INDIVIDUAL	22b. TELEPHONE NUMBER (Include Area Code)	22c. OFFICE SYMBOL

DD FORM 1473, 83 APR — EDITION OF 1 JAN 73 IS OBSOLETE.

Unclassified
SECURITY CLASSIFICATION OF THIS PAGE

structural responses to the loading. The effective driving force for this system is a wavelet that modifies the explosive acoustic source to match the spectral and temporal characteristics of the STS acoustic emissions. A short derivation of the simulation algorithm follows.[4]

The Simulation Algorithm

A pressure load, $d(t,\underline{y})$, applied to a structure at a location defined by the coordinate vector $\underline{y}$, will produce a motion, $u_k(t,\underline{x},\underline{y})$ at some other location specified by the vector $\underline{x}$. The subscript k identifies the component of motion. Assuming the structure behaves as a linear, time invariant system, there exists an impulse response wavelet, $h_k(t,\underline{x},\underline{y})$, connecting the driving load and each component of the induced motions such that

$$u_k(t,\underline{x},\underline{y}) = h_k(t,\underline{x},\underline{y})*d(t,\underline{y})\ \delta A \qquad (1)$$

where δA is the area over which the load is applied and the asterisk represents convolution. The impulse response function is unique in the sense that it is a property of the structure and independent of the loading function, $d(t,\underline{y})$.

Using a superscript S to represent the Shuttle environment and a superscript E for the explosion conditions, equation (1) can be written for the explosion source as

$$u_k^E(t,\underline{x},\underline{y})=h_k(t,\underline{x},\underline{y})*d^E(t,\underline{y})\ \delta A \qquad (2)$$

and for a Shuttle source by

$$u_k^S(t,\underline{x},\underline{y})=h_k(t,\underline{x},\underline{y})*d^S(t,\underline{y})\ \delta A \qquad (3)$$

where $h_k(t,\underline{x},\underline{y})$ is identical in both equations. The equivalent frequency domain representations are

$$U_k^E(f,\underline{x},\underline{y})=H_k(f,\underline{x},\underline{y})D^E(f,\underline{y})\ \delta A \qquad (4)$$

for the explosion and

$$U_k^S(f,\underline{x},\underline{y})=H_k(f,\underline{x},\underline{y})D^S(f,\underline{y})\ \delta A \qquad (5)$$

for the Shuttle launch. The impulse response function, $H_k(f,\underline{x},\underline{y})$ can be evaluated from equation (4) as the spectral ratio of the explosion motions to the explosive driving force, both of which can be obtained empirically. Substituting this quantity into equation (5) yields

$$U_k^S(f,\underline{x},\underline{y})=U_k^E(f,\underline{x},\underline{y})[D^S(f,\underline{y})/D^E(f,\underline{y})]\ \delta A \qquad (6)$$

and relates the observed explosion-induced motions to the STS-induced motions.

Consider the spectral ratio of the driving functions, $[D^S/D^E]$. For a common atmosphere, spherical acoustic propagation is itself a linear, time invariant system. If the explosion and the discrete Shuttle acoustic signals can be represented as propagating from collocated point (monopole) sources, then extrapolation of the pressures from any reference location, specified by the vector $\underline{z}$, to the point of load application can also be shown to be represented in the form of equation (1) or in the spectral domain by

$$D(f,\underline{y},\underline{z})=H^P(f,\underline{y},\underline{z})P(f,\underline{z}) \qquad (7)$$

where $H^P(f,\underline{y},\underline{z})$ is the propagation response function and $P(f,\underline{z})$ is the spectral representation of the pressure wavelet at a location specified by the coordinate vector $\underline{z}$. As before, H^P is independent of the type of source driving the system and the spectral ratio of the driving functions is

$$D^S(f,\underline{y},\underline{z})/D^E(f,\underline{y},\underline{z})=P^S(f,\underline{z})/P^E(f,\underline{y},\underline{z}) \qquad (8)$$

and is solely dependent on the source characteristics, including location, and is independent of the point of load application on the structure.

Substituting equation (8) into equation (6) provides the fundamental relationship between the STS- and explosion-induced motions, or

$$U_k^S(f,\underline{x},\underline{y},\underline{z})=U_k^E(f,\underline{x},\underline{y},\underline{z})[P^S(f,\underline{z})/P^E(f,\underline{z})]\ \delta A \qquad (9)$$

and with conversion into the time domain

$$u_k^S(t,\underline{x},\underline{y},\underline{z})=u_k^E(t,\underline{x},\underline{y},\underline{z})*v(t,\underline{z})\ \delta A \qquad (10)$$

where $v(t,\underline{z})$ is some wavelet, referred to as the driving wavelet, defined by the inverse transform of the spectral ratio of the pressure functions for the STS and the explosion acoustics evaluated at a common reference location.

So far this derivation has treated the motions at $\underline{x}$ due to the load applied at a single point on the surface of the structure specified by the vector $\underline{y}$. In fact, the loads are distributed over the entire surface of the structure and the motions for an STS source, $u_k^S(t,\underline{x},\underline{z})$, are given by the integral of $u_k^S(t,\underline{x},\underline{y},\underline{z})$ over the surface of the structure, or from equation (10)

$$u_k^S(t,\underline{x},\underline{z})=\int u_k^E(t,\underline{x},\underline{y},\underline{z})*v(t,\underline{z})dA. \qquad (11)$$

As $v(t,\underline{z})$ is independent of the load application point, the integral reduces to

$$u_k^S(t,\underline{x},\underline{z})=u_k^E(t,\underline{x},\underline{z})*v(t,\underline{z}) \qquad (12)$$

where $u_k^E(t,\underline{x},\underline{z})$ is the total motion, observed at $\underline{x}$, produced by an explosion along the STS trajectory. This is the actual quantity measured by recording motions produced by a charge detonation.

Equation (12) provides the fundamental algorithm used in this paper to simulate the launch vibration environment at V23. This equation provides the predicted motions at a given location when the Shuttle source is located at the same position as the explosion. To simulate a moving Shuttle source, one need only sum, with appropriate time delays, the motion contributions from each discrete source location.

The Driving Wavelet

What remains, then, is to define the driving wavelet, $v(t,\underline{z})$ used in equation (12). From equation (9), the spectrum of the driving wavelet, $V(f,\underline{z})$, is defined as the spectral ratio of the STS pressure signal to the explosion wavelet at some reference point. It is noted that the derivation given above assumes that both the explosion and the STS acoustic signals can be described as equivalent point sources, at least at each of the discretized source locations.

It is apparent that the acoustic output of a small elevated charge, observed at distances many times larger than the source dimensions, can be represented as emanating from a point source. Further, the acoustic emissions propagate away from the source under the laws governing spherical acoustics. For a flat, perfectly reflecting earth away from obstructions, the explosive pressure wavelet has a spectral form given by

$$P^E(f,r)=(r_c/r)G^E(f,r_c) \qquad (13)$$

where f is frequency, r is the source to observer range, r_c is a reference range, and $G^E(f,r_c)$ is the spectral representation of the pressure wavelet at r_c. The exact form of $G^E(f,r_c)$ is of no consequence in the derivation, however, it was determined empirically and is shown in Figure 2.

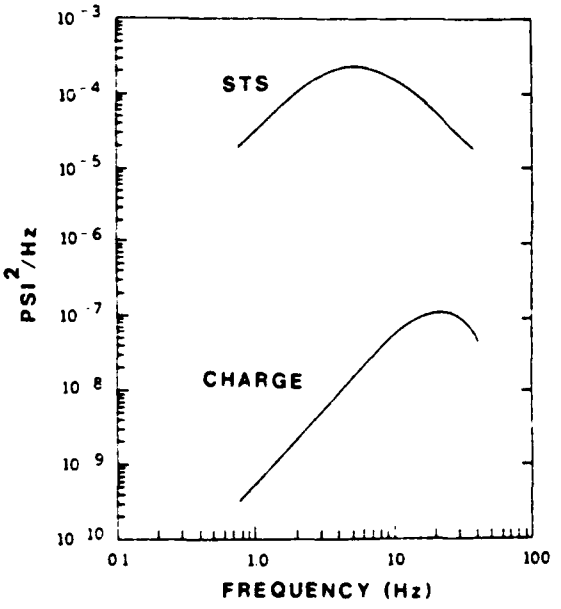

Fig. 2 PSD of charge and STS sources.

It has been shown in previous studies that the acoustics of the STS rocket motor exhaust can also be adequately described at a flat earth site and for limited ranges and azimuths as an axial symmetric source traveling with the rocket but somewhat below it in the exhaust plume.[1,2] For an STS launch, significant acoustic loads are observed at the ground for approximately 30 seconds following main engine ignition. Once clear of the ground, the spectral shape of the acoustic signal remains relatively constant and is well described by a theoretical form proposed by Powell for undeflected, plume generated acoustics.[5] The most significant divergence from this shape occurs early in the launch when the exhaust plume interacts with the ground and during Solid Rocket Booster (SRB) ignition. At these times pressures of concern are low compared with peak values and the change in spectral shape is not expected to greatly affect the forecasted results.

While the spectral shape remains reasonably constant, the level of the spectrum, as observed at a fixed point on the ground, changes throughout the launch. This variation occurs in part as a result of increasing range of the source but, more significantly, due to directivity of the rocket source.[6] For a fixed observer, source directivity and range effects can be equated to a time dependent strength variation.

Mathematically, the STS acoustic pressure spectrum at a fixed point can be modeled as

$$P^S(f,r)=G^S(f,r)[N(f)*E(f,r)] \qquad (14)$$

where r is range from the source, $G^S(f,r)$ is the best fit of the Powell theoretical spectrum to observed STS acoustic spectrum at the time of peak pressure loading, N(f) is the spectrum of a zero mean, unit variance normal process and E(f,r) is the spectrum of an envelope function which provides the correct time dependence of the source strength.

For areas comparable to surface areas of structures at V23, it has been demonstrated that extrapolation of the Shuttle acoustic pressure field from a reference point pressure time history can be adequately made using spherical acoustics.[1,2] Over relatively large areas the STS acoustics can be viewed as having an equivalent point source representation. However, for gross changes in the range or azimuth of interest the functional terms of the point source model must be adjusted. Then, the pressure field about some reference point, r_o, can be given the frequency domain representation of

$$P^S(f,r,r_o)=(r_o/r)G^S(f,r_o)[N(f)*E(f,r_o)] \qquad (15)$$

where r is the range of the point of interest and all other terms are as described above. The Shuttle reference spectrum, $G^S(f,r_o)$, as used for the PDF simulations, is also shown in Figure 2.

This model replaces the moving STS acoustic source with a single, stationary source representation. It should be noted that potentially significant information on the temporal variation of the pressure phasing on structures is lost in this approximation. However, it will be shown in a later section that this effect does not degrade the forecasts beyond levels imposed by other factors in the simulation process.

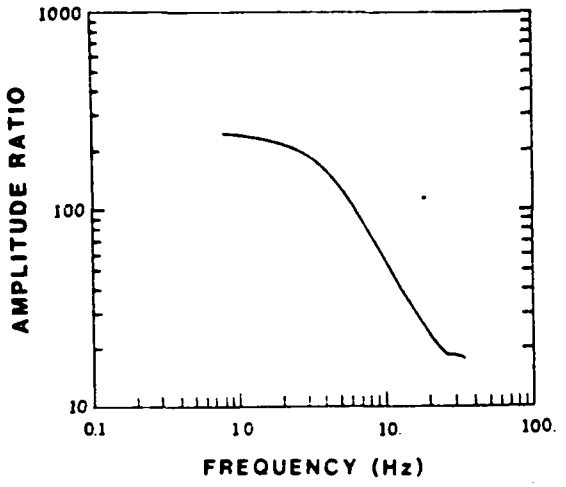

Fig. 3 Spectrum of the shaping wavelet, $W(f,r_o)$.

From equations (13) and (15), the spectral driving function, $V(f,r)$ is given by

$$V(f,r)=[G^S(f,r_o)/G^E(f,r_o)][N(f)*E(f,r_o)] \quad (16)$$

under the conditions that $G^S(f,r_o)$ and $G^E(f,r_o)$ are evaluated under the same boundary conditions and at the same reference range. Under this condition, the range dependence of $V(f,r)$ is reduced to a dependence on the reference range, r_o.

Defining the ratio of the G functions to be the shaping spectrum, $W(f,r_o)$, and the inverse transform to be the shaping wavelet, $w(t,r_o)$, then the driving function is

$$v(f,r_o)=w(t,r_o)*[n(t)e(t,r_o)] \quad (17)$$

The theoretical form used for $G^S(f,r_o)$ in this study does not provide the phase information required to perform the inverse transformation of $W(f,r_o)$. This requirement is met by specifying that the operator $w(t,r_o)$ be realizable and of minimum phase. The PSD of the shaping wavelet, $W(f,r_o)$, as used for the PDF predictions is shown in Figure 3 and Figure 4 shows the envelope function, $e(t,r_o)$ used in the simulations.

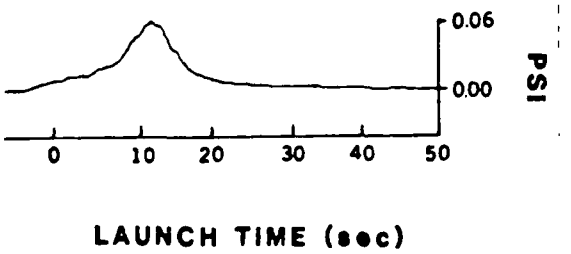

Fig. 4 STS acoustic envelope function, $e(t,r_o)$.

The Simulation Equation

Combining equations (12) and (17) provides the formulation used in this study to simulate the vibration environment at selected locations in GSS facilities during an STS launch. This construction is given by

$$u_k^S(t,\underline{x},\underline{z})=u_k^E(t,\underline{x},\underline{z})*w(t,r_o)*[n(t)e(t,r_o)]. \quad (18)$$

Simulations made with this algoritm are based primarily on a peak load regime and largely ignore dynamic pressures and ground cloud attenuation. It is reiterated that this construction ignores the movement of the Shuttle acoustic source and substitutes a single fixed source. In addition, simulations were made for a typical Shuttle trajectory and for the standard Shuttle propulsion system without thrust augmentation.

Verification of the Method

A problem similar to the one at hand is that of forecasting motions induced in buildings by the infrasonic emissions of a Hush House, a jet engine ground run-up noise suppressor. Both the Shuttle and the Hush House acoustic emissions are plume generated. Figure 5 shows observed and simulated vibrations in a structure approximately 300 meters from the Luke AFB Hush House during the run-up of an F-100 engine. The simulated motions were generated in a manner similar to the method just described. The motions produced by a small explosive charge located near the Hush House were combined with observed low frequency emissions of the Hush House to produce the forecast motions. The simulation accurately reproduces the observed trace. Discrepancies between the two signals can readily be explained as resulting primarily from differences in the explosion and Hush House source locations. This test verifies the concept of simulating acoustic-induced motions based on explosion responses.

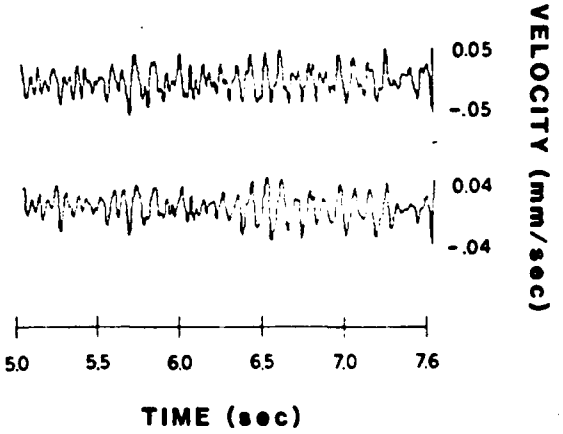

Fig. 5 Observed (upper) and predicted (lower) motions due to a Hush House acoustic source.

IV. The Sounding Program

In January of 1984, an explosive Sounding Program was conducted at V23. During this study, a series of small charges were detonated over the V23 Launch Mount and the induced motions recorded at locations in several GSS facilities. These observ-

ations provide the $u_k^E(t,\underline{x})$ term for use in the simulation algorithm. A total of eight three-component sensor installations were used during the Sounding Program.

The charges were suspended at elevations of 15, 46 and 58 meters above the Launch Mount; elevations comparable to the first 7 seconds of the Shuttle trajectory. Physical limitations on charge placement restricted the maximum elevation used in the Sounding Program. The maximum charge elevation was limited by the height of a suspended line between the SAB and the MST. All structures were in launch configuration at the time of the Sounding Program. However, exterior sheathing had not been installed on the SAB at that time and, it can be expected that the completion of this structure would alter the forecasted motions to some degree.

All vibration measurements were made using an element of the AFGL Geophysical Data Acquisition System (GDAS).[7] Individual channel responses were determined by analyzing the transients excited by a step input, with sensors in place, before and after each shot sequence. A typical system response function for seismic measurements is shown in Figure 6. Forecasts were made for the frequency band of 0.4 to 30 Hz.

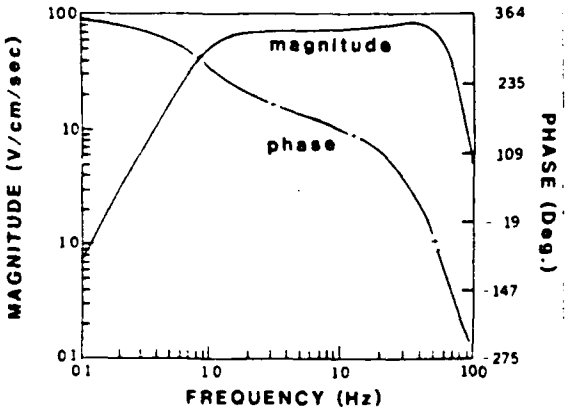

Fig. 6 A typical GDAS system response for motion measurements.

The repeatability of the explosion-induced motions is shown in Figure 7. This figure shows the Power Spectral Density (PSD) functions for two shots at the same elevation and observed at the same location. Below 30 Hz the two spectra duplicate the major features of the building response. Significant variations exist above 30 Hz but these can be explained by slight shifts in the source location or wind effects. In any case, the vibration forecasts are essentially band limited to 0.4 to 30 Hz.

Figure 8 shows the PSD functions obtained for the PPR at Level 99 on the east-west component of motion for the 15 and 46 meter shots recorded at this site. While some differences are noted in the spectra below 30 Hz, the major elements remain reasonably constant. It appears that the structural responses, at least over the range of shot elevations used, are insensitive to source height. This behavior was found to be consistent for all components and at all locations studied during the Sounding Program. This fact justifies the use of a fixed source for the Shuttle acoustics in the prediction procedure.

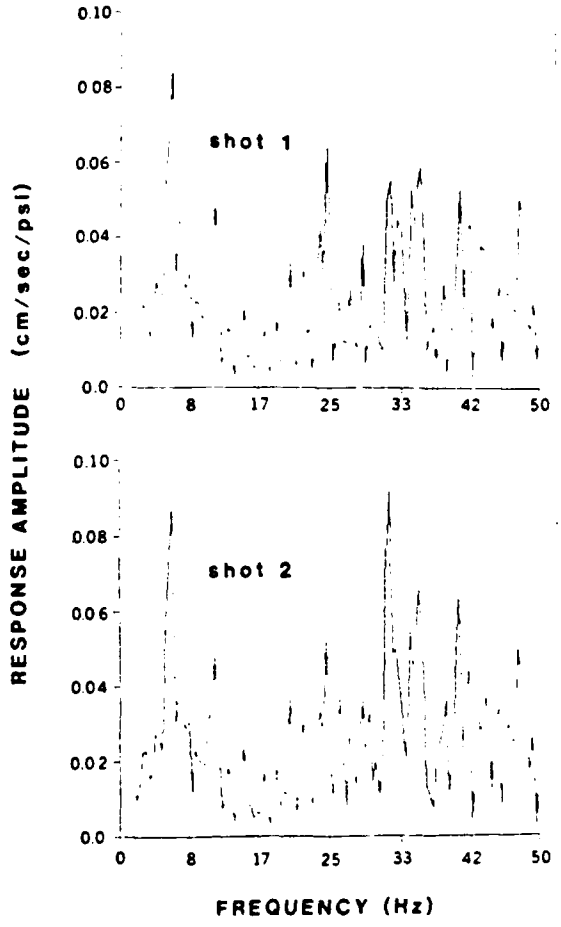

Fig. 7 PPR motion response for two shots at the same elevation.

V. Launch-Induced Vibration Forecasts

Following the procedure given above, simulations of the Shuttle launch-induced vibrations at V23 were made for each of the eight locations instrumented during the Sounding Program. Multiple simulations were made for each location by using distinct realizations of the normal process, n(t), to drive the algorithm. In the following sections the forecasts for each structure are discussed.

The Payload Preparation Room

Five locations were studied in Checkout Cell 2 of the PPR. Sensors were located at the cell rail to platform connection at Levels 119 and 99 and on the footings of the cell rails at Level 69. It is anticipated that payloads for subsequent launches will be located in the PPR Checkout Cells during any given launch and, therefore, specific criteria

have been established for the motion environment in the cells. These criteria are equivalent to a requirement that RMS accelerations in the band 0.4 to 30 Hz not exceed 0.5 g.

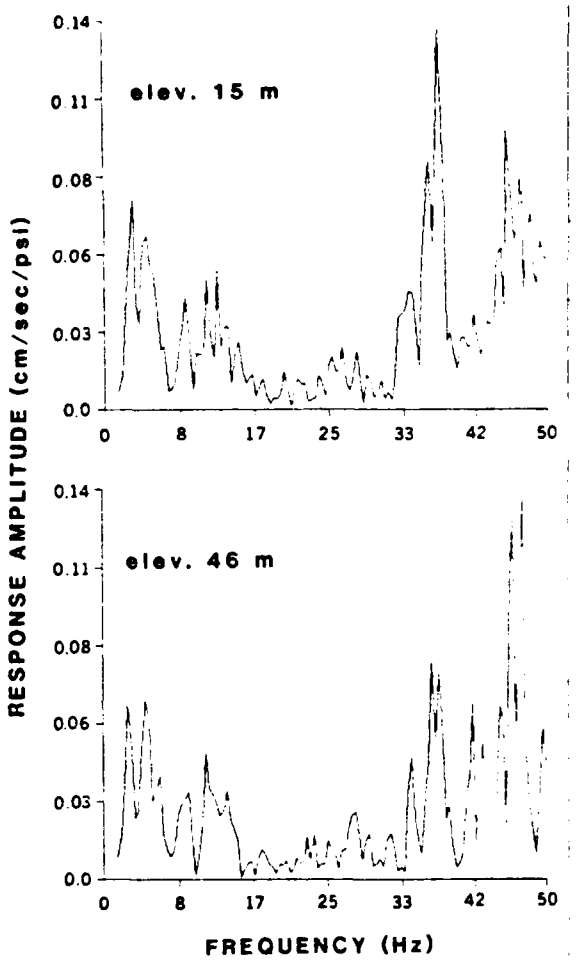

Fig. 8 PPR motion responses for two shots at different elevations.

As would be expected, the highest motions forecast in the PPR occurred at Level 1'9 (Figure 9) and peak accelerations were almost an order of magnitude less than the stated criteria for RMS values. The present results are typically much less than the vibration forecasts made using Finite Element modeling of the launch conditions in the PPR.[5] Based on statistical properties of the forecasted motions and given the restrictions on the forecast methodology, an acceleration of 0.06 g will not be exceeded at any measurement point in the PPR with a confidence level of 99%.

However, it is likely that higher than forecasted motions will be observed in the PPR. As the Shuttle rotates and moves to the south of the Launch Mount it is anticipated that the pressure loading on the PPR will increase. In addition, response characteristics of the PPR indicate that it is more responsive to loading in a north-south direction than along the east-west axis. Due to physical restrictions on the placement of the explosive source this situation could not be investigated during the Sounding Program. It is not believed, however, that this effect will greatly increase the acceleration levels in the structure.

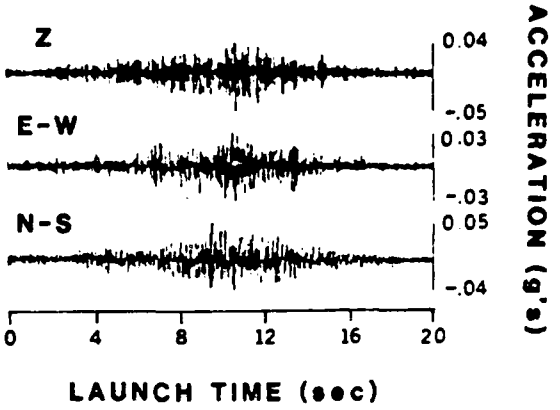

Fig. 9 Simulated accelerations for Level 1'9 in the PPR.

One question that has been raised throughout the V23 project has been the import of acoustic coupled seimic vibrations during launch at structures such as the PPR and the Launch Control Center (LCC). Although the Sounding Program did not simulate the conditions likely to generate the largest seismic signal during a launch, when the Shuttle exhaust is being vented through the flame duct, it does provide some indication of the seismic excitation level that could be anticipated. At each charge elevation, seismic precursors were recorded prior to the direct acoustic excitation of the structure. In all cases, the seismic arrivals were no more than 10% of the acoustic-induced motions. This suggests that construction of the PPR underground, as originally planned, would have resulted in a significantly lower launch-induced vibrations environment in the PPR.

The Administration Building

One three-component seismometer station was located on the floor of the Orbiter Functional Simulator (OFS) Room of the Administration Building. This room will contain computer equipment used to simulate orbiter operations in a post-launch situation. It is our understanding, however, that this equipment will not be operating during the launch.

Vertical accelerations at this location will approach, and might easily exceed, 1 g. Horizontal peak accelerations are significantly lower, typically about 0.'5-g. Actual forecast amplitudes for the vertical motions exceed 0.7 g (Figure 1'). As with the PPR, however, as the Shuttle climbs and rotates to the south, pressure loading on the AB will increase and, as a consequence, accelerations at this location can also be anticipated to exceed the forecasted values.

It is known that the computer equipment to be

installed in the OFS Room has been tested only to a 1.0 g level. The capabilities of the equipment to withstand higher accelerations has apparently not been demonstrated. Further, building responses involving vertical accelerations approaching 1 g are typically considered unacceptable. However, with only one study location in the AB it is not possible to determine if this behavior is a localized event or symtomatic of a structural problem.

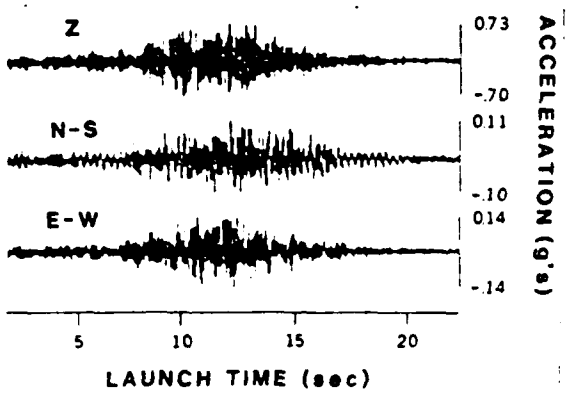

Fig. 10 Simulated Motions in the OFS Room.

The Payload Changeout Room

The PCR is a mobile structure in which the Shuttle payloads are transferred from the PPR to the Shuttle at the Launch Mount. In launch configuration, the PCR will be parked within inches of the PPR. During the Sounding Program, two sites were monitored in this facility. The sensors were located on the upper and lower Payload Ground Handling Mechanism (PGHM) rails at Platforms 6 and 11 in the PCR.

Figure 11 displays the simulated motions for the upper PGHM rail location. For a source located over the Launch Mount, the PCR exhibits lightly damped sway in the east-west direction. Extrapolation of the westward sway displacements forecasted for Platform 12 to the top of the building indicate that pounding of the PCR and PPR is a distinct possibility. Pounding between the two structures could result in unpredictably high accelerations in both the PPR and PCR and, potentially, structural damage to either or both buildings.

The probability of pounding depends on the actual separation of the structures at launch. Figure 12 shows the probability distribution for peak westward (towards the PPR) displacement of the PCR in terms of duration of steady state motions. Repeated measurements of the separation between the PPR and PCR in park position have shown the separation to be no more than 4 centimeters, indicating that, on average, pounding will occur once in every 20 to 30 launches. It should be noted that sway in the PPR transfer tower has not been considered in this forecast. Motion in this structure will only increase the probability of pounding. For example, if the transfer tower of the PPR and the PCR have equal but out of phase displacements, the probability of pounding increases to almost 60%. It has been suggested that the PPR-PCR separation can be increased to over 7 centimeters in which case the likelihood of pounding becomes negligible.

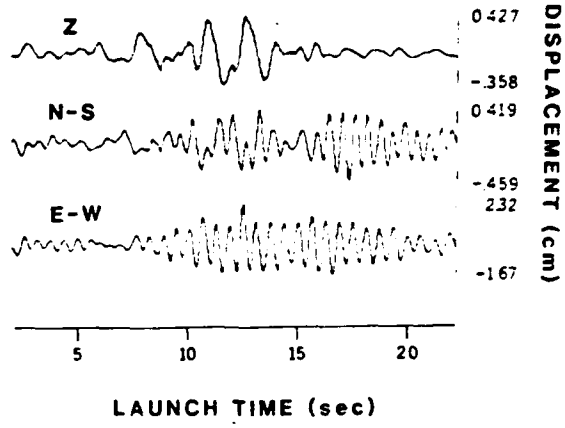

Fig. 11 Simulated Motions for the upper PGHM Rail of the PCR.

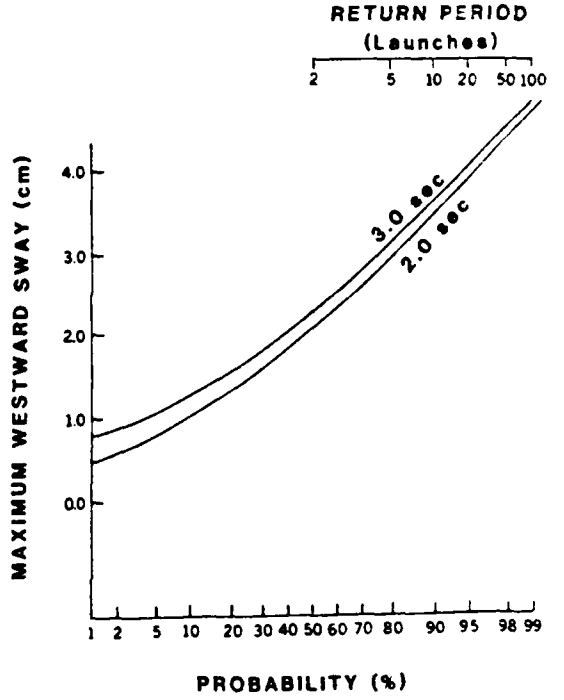

Fig. 12 Probability distribution of the maximum westward displacement of the PCR.

References

1. Crowley, F. A., Hartnett, E. B. and Ossing, H. A. (1983) Amplitude and Phase of Surface Pressure Produced by Space Transportation Systems Mission 5, AFGL-TR-83-0039, Boston College.

2. Crowley, F. A., Hartnett, E. B. and Fisher, M. A. (1984) Surface Pressure Produced by Space Transportation System Flight 41B, AFGL-TR-84-0213, Boston College.

3. Crowley, F. A., and Hartnett, E. B. (1984) Vibro-Acoustic Forecast for the Space Shuttle Launches at Vandenberg AFB, The Payload Change-out Room and the Administration Building, AFGL-TR-84-0322, Boston College.

4. Battis, J. C. (1985) Vibro-Acoustic Forecasts for STS Launches at V23, Vandenberg AFB: Results Summary and the Payload Preparation Room, AFGL-TR-85-0133, Air Force Geophysics Laboratory.

5. Powell, A. (1964) Theory of Vortex Sound, Jour. Acoustic Soc. of Amer., 36, pp 177-195.

6. Crowley, F. A. Hartnett, E. B., and Ossing, H. A. (1980) The Seismo-Acoustic Disturbances Produced by a Titan III-D with Application to the Space Transportation System Launch Environment at Vandenberg AFB, AFGL-TR-80-0312, Air Force Geophyics Laboratory.

7. von Glahn, P. (1980) The Air Force Geophysics Laboratory Standalone Data Acquisition System: A Functional Description, AFGL-TR-80-0317, Air Force Geophysics Laboratory.

8. Yang, R. C. and Teegarden, W. T. (1980) Part III, Vibro-Acoustic Study, Payload Preparation Room Summary, VRC-79-145, Martin Marietta Corp.